Hydrogel films and coatings by swelling-induced gelation

David Moreau[a,b], Caroline Chauvet[c,d], François Etienne[c,d], François P. Rannou[c,d,e], and Laurent Corté[a,b,1]

[a]MINES ParisTech, Paris Sciences et Lettres Research University, Centre des Matériaux, CNRS UMR 7633, 91003 Evry, France; [b]ESPCI Paris, Paris Sciences et Lettres Research University, Laboratoire Matière Molle et Chimie, CNRS UMR 7167, 75005 Paris, France; [c]INSERM, UMR-S 1124, 75270 Paris Cedex 06, France; [d]Université Paris Descartes, Sorbonne Paris Cité, Paris 75006, France; and [e]Université Paris Descartes, Pôle de Recherche et d'Enseignement Supérieur Sorbonne Paris Cité, Service de Rééducation et Réadaptation de l'Appareil Locomoteur et des Pathologies du Rachis, Hôpital Cochin, Assistance Publique–Hôpitaux de Paris, 75014 Paris, France

Edited by David A. Weitz, Harvard University, Cambridge, MA, and approved October 3, 2016 (received for review June 14, 2016)

Hydrogel films used as membranes or coatings are essential components of devices interfaced with biological systems. Their design is greatly challenged by the need to find mild synthesis and processing conditions that preserve their biocompatibility and the integrity of encapsulated compounds. Here, we report an approach to produce hydrogel films spontaneously in aqueous polymer solutions. This method uses the solvent depletion created at the surface of swelling polymer substrates to induce the gelation of a thin layer of polymer solution. Using a biocompatible polymer that self-assembles at high concentration [poly(vinyl alcohol)], hydrogel films were produced within minutes to hours with thicknesses ranging from tens to hundreds of micrometers. A simple model and numerical simulations of mass transport during swelling capture the experiments and predict how film growth depends on the solution composition, substrate geometry, and swelling properties. The versatility of the approach was verified with a variety of swelling substrates and hydrogel-forming solutions. We also demonstrate the potential of this technique by incorporating other solutes such as inorganic particles to fabricate ceramic-hydrogel coatings for bone anchoring and cells to fabricate cell-laden membranes for cell culture or tissue engineering.

hydrogel film | hydrogel coating | associative polymers | cell culture | tissue engineering

Hydrogel films are used in a number of biomedical applications like wound healing (1), drug delivery (1), antiadhesive membranes (2), soft-tissue reconstruction (3, 4), and cell culture (5). The quality of their interactions with biological tissues or entrapped cells is central to the performance of these systems. Although considerable advances have been made in synthesis (6) and processing (7) to tailor these interactions, the toxicity of by-products and the degradation caused by harsh processing conditions remain key issues (8), which can be overcome (9) but are often addressed at the cost of difficult synthesis or multistep processes. There is a great interest for simple, versatile, and in vivo-friendly methods to fabricate and modify hydrogels. We propose a strategy to design hydrogel films in mild conditions. This method could be used to produce free-standing hydrogel membranes or hydrogel coatings to functionalize other hydrogels.

Our approach relies on the understanding of transport phenomena occurring near the surface of a polymer network swelling in a polymer solution. As an illustration, let us consider a flat polymer network with thickness H_0 immersed in a solution containing a volume fraction Φ_0 of free polymer chains, as depicted in Fig. 1*A*. When the solvent of the solution is also a solvent for the network, the network swells in a diffusive process. For early immersion times t, the increase in thickness ΔH is given by the following (10, 11):

$$\Delta H = (H_\infty - H_0)\frac{(D_0 t)^{1/2}}{H_0}, \qquad [1]$$

where H_∞ is the thickness at equilibrium swelling in the polymer solution and D_0 is a diffusivity coefficient depending on the dynamics of the network and of the solution. The systems of interest are those where the chains in solution do not penetrate the network during swelling, for example, for chains that are much larger than the network mesh size. In this case, free chains are pushed away by the swelling network, which creates an opposite flux of solvent into the network. As a result, a volume $V \sim \Phi_0 \Delta H$ of free chains accumulates near the network surface and is redistributed by thermal diffusion within a layer of thickness $d \sim (D_s t)^{1/2}$, where D_s is the diffusivity coefficient of free polymer chains in the solution. The excess in polymer concentration averaged over this layer thus scales as $V/d \sim \Phi_0((H_\infty - H_0)/H_0)(D_0/D_s)^{1/2}$. For polymer gels, the ratio $(H_\infty - H_0)/H_0$ is typically between 1 and 10. Therefore, with a proper selection of the diffusivity ratio D_0/D_s, the concentration of a polymer solution might be amplified manyfold near the surface of a swelling polymer network. In particular, this regime might be achieved with solutions of associative polymers, in which diffusivity decays strongly with concentration. For instance, strong concentration gradients were reported at the surface of polyelectrolyte gels swelling in a solution of (hydroxypropyl)cellulose (12). Here, we propose to exploit this solvent depletion induced by swelling to produce hydrogel films and coatings in a soft and autonomous manner.

The generic idea of our approach is depicted in Fig. 1*B*. It uses the property of some aqueous polymer solutions to form physical gels at high concentration. First, a substrate composed of a dry hydrophilic network is immersed into such a solution (*i*). As described above, substrate swelling causes the polymer concentration to increase in a layer near the substrate surface (*ii*). At a given level of swelling, this layer becomes so concentrated that free polymer chains associate and form physical cross-links (*iii*).

Significance

This work reports a processing route to fabricate hydrogel films through their rapid and spontaneous growth in aqueous solutions. This approach exploits the strong solvent depletion created at the surface of a polymer substrate swelling in a polymer solution. By immersing substrates that swell in associative polymer solutions, we showed that this local suction effect induces the gelation and growth of hydrogel films. Experiments and a simple model captured how the kinetics of this process can be deliberately controlled by handy processing parameters. Other solutes can be easily incorporated in the so-formed hydrogel films to provide other functionalities. We demonstrated this potential by coating complex shapes with bioceramic particles and by encapsulating mammalian cells in freestanding membranes.

Author contributions: D.M., C.C., F.P.R., and L.C. designed research; D.M., C.C., F.E., and L.C. performed research; D.M., C.C., and L.C. analyzed data; and D.M., C.C., F.P.R., and L.C. wrote the paper.

The authors declare no conflict of interest.

This article is a PNAS Direct Submission.

[1]To whom correspondence should be addressed. Email: laurent.corte@mines-paristech.fr.

This article contains supporting information online at www.pnas.org/lookup/suppl/doi:10.1073/pnas.1609603113/-/DCSupplemental.

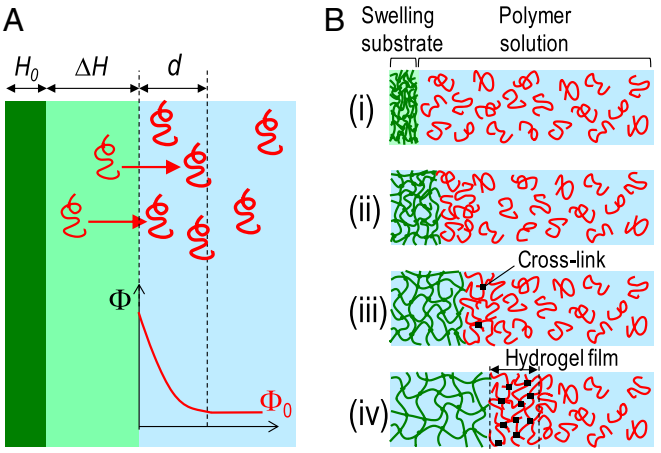

Fig. 1. Formation of hydrogel films by swelling-induced gelation. (*A*) Schematic representation of the solvent depletion created near the surface of a swelling polymer network. Upon immersion in a polymer solution, the dry network (dark green) swells. Free polymer chains (red) are pushed away from the volume spanned by the swelling network (light green) and accumulate near its surface. This creates a local excess in polymer concentration in the solution, which is redistributed by thermal diffusion. (*B*) Illustration of the design strategy using swelling of a hydrophilic polymer substrate to induce the formation of hydrogel films.

As swelling proceeds, the cross-linking density increases until the gel point is reached and a hydrogel film is formed at the surface of the substrate (*iv*).

Aqueous solutions of associative polymers forming thermoreversible gels are good candidates to fabricate hydrogel films by the proposed method. In particular, we concentrate on poly(vinyl alcohol) (PVA), which undergoes a sol–gel transition in water at 20 °C for concentrations between 20 and 40 wt% (13, 14). This gelation results from the physical cross-linking of PVA chains that associate through hydrogen bonds and form crystallites (14). For high-enough cross-linking densities, the so-formed PVA hydrogels remain stable below the melting temperature of PVA crystallites, which can reach 80–90 °C. Practically, physical PVA hydrogels show a good biocompatibility, which makes them of high interest to the biomedical field. They have been widely studied as a constitutive material for biomembranes (15, 16), cell encapsulation (17, 18), or soft-tissue reconstruction (4, 19). In that respect, several methods have been developed to induce the gelation of PVA, using solvent evaporation (20), thermal treatments by freezing–thawing (19), coagulation in poor solvent (15), or salting out (21).

Results and Discussion

Formation of Hydrogel Films Induced by Swelling. The formation of PVA hydrogel films induced by the swelling of a polymer substrate was demonstrated with a simple experiment described in Fig. 2*A* and Movie S1. Substrates consisted of 3-mm-thick films of covalently cross-linked poly(acrylamide) (PAAm). In water, they normally swell and reach equilibrium within 90 h to form 6-mm-thick hydrogel films. In this experiment, dry PAAm films were immersed in a 15 wt% PVA aqueous solution for 3 h and were then vigorously rinsed in water for 15 min. Films of PVA hydrogel could be peeled off from the substrates immediately after rinsing (Fig. 2*B*). These films remained insoluble in water at 20 °C for over a week (Fig. 2*C*) but dissolved in less than 1 h at 90 °C (Fig. 2*D*). This confirms that physical PVA hydrogels were formed, for which cross-linking crystallites melt in water above 85 °C (22, 23). Accordingly, the formation of PVA crystallites in these films was verified by X-ray scattering, which revealed the main Bragg peak of PVA crystals (Fig. S1).

Characterization of Hydrogel Film Growth as a Function of Substrate Swelling. The relationship between substrate swelling and hydrogel film formation was investigated in other experiments, as illustrated in Fig. 3*A*. Spherical substrates were immersed in aqueous solutions and were observed from the top to monitor both substrate swelling and hydrogel film formation. Spheres of poly(acrylic acid)–poly(acrylamide) (PAAc–PAAm) hydrogels containing a green dye were used as the swelling substrates (Fig. 3*B*). These dry spheres had a radius of 1.20 ± 0.05 mm. During swelling in pure water, a sharp line at the sphere equator indicated the substrate–water interface, as shown in Fig. 3*C* for 1-h immersion. Equilibrium swelling was reached in 400 min with a radius of 13.0 ± 0.1 mm.

The growth of PVA hydrogel films induced by swelling was observed when the dry spheres were immersed in PVA solutions. In those cases, a second larger circle appeared concentric with the substrate equator, as shown in Fig. 3 *D* and *F* for 10 wt% PVA solutions (Fig. S2 for other concentrations). This line corresponds to the interface between the solution and a PVA hydrogel film, as seen when detaching the film under the microscope (Fig. S3 and Movie S2). The film thickness was measured from the radius difference between the two circles (Fig. S4). Control experiments confirmed that film formation was induced by swelling. For that, PAAc–PAAm spheres were swollen to equilibrium in pure water before immersion in a 10 wt% PVA solution. As expected, osmotic deswelling was observed after immersion in the PVA solution (24) but no hydrogel film was noticed, as shown in Fig. 3*E* for 1-h immersion.

Fig. 4*A* shows the increase in radius of PAAc–PAAm spheres as a function of immersion time in solutions with PVA concentrations ranging from 0 to 15 wt%. Swelling decreased with increasing PVA concentration because of the osmotic pressure created by free PVA chains. For all of the studied concentrations, the curves were well fitted by Eq. **1**. The diffusivity, D_0, obtained from these fits is plotted in Fig. 4*B*. It drops sharply as the PVA concentration increases above the overlap concentration ($C^* = 2.6$ wt%) (25). This transition suggests that, in the semidilute regime, the slow relaxation of overlapping PVA chains is the limiting process that dictates the kinetics of substrate swelling.

Fig. 4*C* shows the thickness of hydrogel films formed at the surface of the spheres as a function of immersion time. These

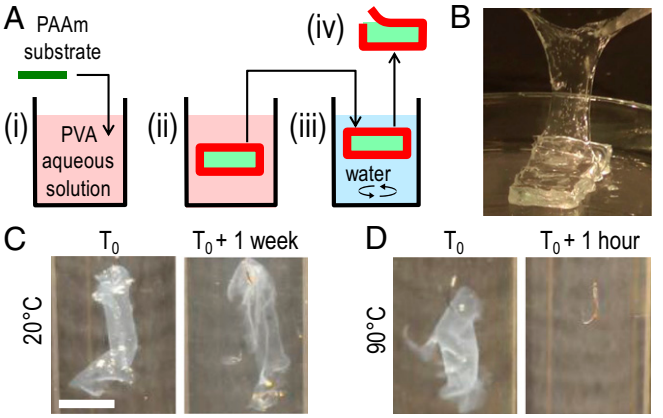

Fig. 2. Formation of PVA hydrogel films on swelling PAAm substrates. (*A*) Schematic representation of the experimental protocol: (*i*) a dry PAAm substrate is immersed in a PVA aqueous solution; (*ii*) the PAAm substrate swells inducing the formation of a PVA hydrogel film (dark red); (*iii*) the sample is collected and rinsed in water; (*iv*) the PVA hydrogel film can be peeled off from the swollen PAAm substrate. (*B*) Peeling of a PVA hydrogel film after 3-h immersion in a 15 wt% PVA aqueous solution. (*C* and *D*) Stability in water of the same films as in *B*: right after fabrication (*C* and *D*, *Left*) and after storage at 20 °C for 1 wk (*C*, *Right*) or after storage at 90 °C for 1 h (*D*, *Right*). (Scale bar: 1 cm.)

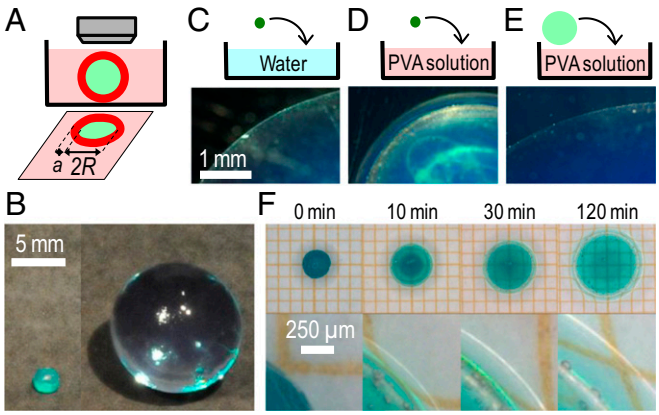

Fig. 3. Observation of hydrogel film growth. (*A*) Schematic representation of the experimental setup enabling the simultaneous observation of the size of the substrate (light green) and of the thickness of the hydrogel film (dark red). (*B*) Spherical PAAc–PAAm substrates: dry (*Left*) and swollen to equilibrium in water (*Right*). (*C–E*) Pictures of the equatorial region of PAAc–PAAm spheres after 1-h immersion in different conditions: the sphere is immersed dry in water (*C*); the sphere is immersed dry in a 10 wt% PVA solution, which reveals the formation of a PVA hydrogel film (*D*); the sphere is first swollen to equilibrium in pure water and then immersed in a 10 wt% PVA solution (*E*). (*F*) Time series of a PAAc–PAAm sphere swelling in a 10 wt% PVA solution: substrate swelling (*Top*) and close-up showing film growth at the sphere surface (*Bottom*).

results depend strongly on the solution concentration. In the dilute regime (1 wt%), no film was observed. Close to the overlap concentration (2.5 wt%), the formation of a 40-μm-thick film was noticed after 10 min, which may correspond to an incubation time or to the detection limit of our technique. In the semidilute regime (≥5 wt%), a film was detected within the first 100 s. For a given immersion time, higher PVA concentrations produced thicker films. In all cases, the thickness growth obeys a power law close to $t^{1/2}$, as shown in Fig. 4*D*.

Mechanisms and Modeling of Swelling-Induced Gelation. A microscopic picture explains the mechanisms of film growth. At the beginning of immersion in a PVA solution, the gelation of a PVA layer is induced by swelling as depicted in Fig. 1*B*: (*i* and *ii*) the PVA concentration increases near the surface of the swelling substrate; (*iii*) PVA chains cross-link by crystallization in this concentrated layer; (*iv*) above a critical gelation concentration Φ_c, a hydrogel film is formed. At this stage, a new regime is expected. Extraction of water from the newly formed hydrogel film into the substrate becomes difficult because it implies an elastic deformation of the cross-linked PVA network. Instead, it becomes more favorable for water to flow from the solution through the hydrogel film and into the substrate, as already described for gel membrane permeation (26). As a result, the solvent depletion process is displaced at the interface between the hydrogel film and the solution. The film builds up continuously through this process until substrate swelling no longer generates a concentration exceeding the gelation concentration.

A simple model based on this picture captures quantitatively the kinetics of film growth. Let us consider that, after an immersion time t, a PVA hydrogel layer of thickness a is formed, as illustrated in Fig. 5*A*. The solution is in large excess and the PVA concentration far from the substrate remains constant, equal to Φ_0. We assume that the hydrogel layer is homogeneous with a constant PVA concentration equal to Φ_c and that the PVA concentration decreases sharply from Φ_c to Φ_0 in a negligible transition layer near the hydrogel surface. This latter assumption is supported by the measured values of substrate diffusivity D_0, which are much larger than the values reported for the diffusivity of PVA in semidilute aqueous solutions, $D_s < 10^{-8}$ cm^2/s (27). In other words, the swelling surface advances much faster than the spreading of concentration fluctuations in the solution. Mass conservation implies that the amount of PVA pushed away during swelling is equal to the excess in PVA in the hydrogel film. This writes simply as follows:

$$\Phi_0 V_s = (\Phi_c - \Phi_0) V_f, \qquad [2]$$

where V_s is the volume spanned by the substrate during swelling and V_f is the volume of the film. Combination with Eq. **1** gives the expression for the hydrogel film thickness as a function of immersion time, for 1D swelling of a flat substrate with initial thickness H_0:

$$a(t) = \left(\frac{\Phi_0}{\Phi_c - \Phi_0}\right)\left(\frac{H_\infty - H_0}{H_0}\right)(D_0 t)^{1/2}, \qquad [3]$$

and for swelling of a spherical substrate with initial radius R_0 (see calculation details in *SI Materials and Methods*):

$$a(t) = R_0\left\{\left[\frac{\Phi_c}{\Phi_c - \Phi_0}\left(1 + \frac{R_\infty - R_0}{{R_0}^2}(D_0 t)^{1/2}\right)^3 - \frac{\Phi_0}{\Phi_c - \Phi_0}\right]^{1/3} - \left(1 + \frac{R_\infty - R_0}{{R_0}^2}(D_0 t)^{1/2}\right)\right\}, \qquad [4]$$

where H_∞ and R_∞ are the thickness and the radius of the substrate at equilibrium swelling in the PVA solution, respectively.

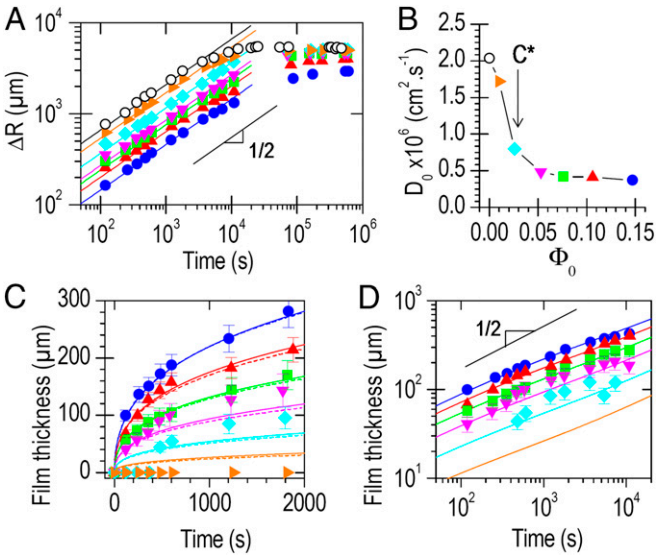

Fig. 4. Relationship between substrate swelling and hydrogel film growth. (*A*) Increase in the radius of PAAc–PAAm spheres as a function of immersion time in aqueous solutions with different PVA concentrations: 0 wt% (○), 1 wt% (▸), 2.5 wt% (◆), 5 wt% (▼), 7.5 wt% (■), 10 wt% (▲), and 15 wt% (●). Full lines show best fits by Eq. **1** for the first hour of swelling. (*B*) Substrate diffusivity measured from fits as a function of PVA concentration. The overlap concentration C* indicates the transition from dilute to semidilute PVA solutions. (*C*) Thickness of PVA hydrogel films as a function of immersion time for the same experiments as in *A*. Full lines show model predictions with Eq. **4** for a spherical substrate (Φ_c = 0.35 wt%). Dashed lines show the results of numerical simulations. (*D*) Same as *C* in log-log scale. In all graphs, error bars represent the maximum SD in a time series. They are not shown when smaller than the symbols.

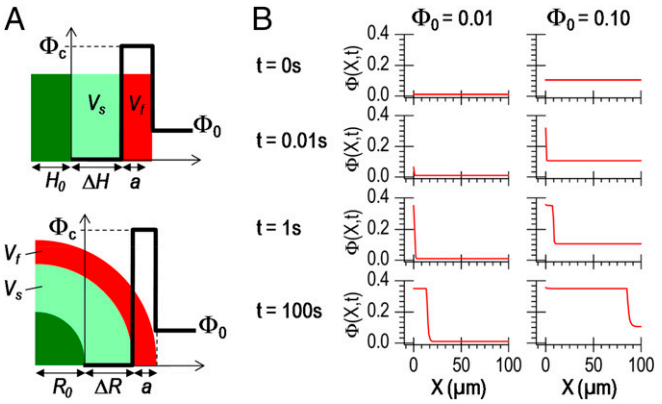

Fig. 5. Modeling of swelling-induced gelation. (*A*) Schematic representations of the analytical model predicting hydrogel film growth for 1D swelling (*Top*) and for swelling of a spherical substrate (*Bottom*). (*B*) Calculated concentration profiles as a function of the distance from the substrate surface at different times during swelling for two initial polymer concentrations: 1 vol% (*Right*) and 10 vol% (*Left*).

The prediction of Eq. **4** is applied to fit the experimental data with Φ_c as the only adjustable parameter and using the experimental values for D_0 given in Fig. 4*B*. For concentrations greater than 5 wt%, an excellent agreement between model and experiment is obtained with $\Phi_c = 0.35$ (full lines in Fig. 4 *C* and *D*). This is consistent with the value of 30 ± 10 wt% reported for the gelation concentration of PVA in water at 20 °C (13, 28). These results demonstrate that film growth can be tailored by adjusting the properties of the solution (Φ_0, Φ_c) and substrate (R_0) as well as the swelling parameters (R_∞, D_0), all of which are well characterized by standard techniques.

A more microscopic insight is given by numerical simulations. For that, we adapted a model of mass transport near an interface, where diffusion and convection are decoupled (29). The model was implemented for a spherical substrate swelling in a polymer solution. Substrate swelling and polymer diffusion in the solution are characterized by constant diffusivities D_0 and D_s, respectively. A discrete profile $\Phi(X,t)$ describes the polymer concentration in the solution at time t between a distance X and $X + \Delta X$ from the substrate surface. The origin ($X = 0$) is attached to the moving substrate surface. We define a as the thickness of the hydrogel film formed at the surface of the substrate. Simulations started from a solution with uniform polymer concentration Φ_0 and with no hydrogel film at the surface of the substrate ($a = 0$).

Between each time step t and $t + \Delta t$, the increase in substrate radius ΔR due to swelling was calculated from Eq. **1** and the origin ($X = 0$) was translated by ΔR. The accumulation of free polymer chains in solution near the surface of the substrate was simulated by injecting at $X = 0$ (or $X = a$ if a hydrogel film is formed) the polymer chains that were pushed away during swelling. The concentration profile was then equilibrated by taking into account the coordinates moving with the substrate surface and by applying Fick's law in the solution. The formation (respectively, growth) of a hydrogel film was simulated by following the solution concentration at the substrate (respectively, hydrogel film) surface: $\Phi(X = a,t)$. Whenever $\Phi(X = a,t) \geq \Phi_c$, the solution near the swelling surface was considered to be gelled in a layer of thickness ΔX. In that case, the volume of the hydrogel film was increased by adding the gelled layer to it and the value of a was updated. A more detailed description of the calculations is given in *SI Materials and Methods*.

Simulations were performed with the same values for R_0, R_∞, and D_0 as those measured experimentally with PAAc–PAAm spheres swelling in PVA solutions. The collective diffusivity of PVA in water decreases strongly with concentration. For the sake of simplicity, an upper bound value was taken as $D_s = 2.10^{-8}$ cm^2·s^{-1} (27). The critical gelation concentration was taken as $\Phi_c = 0.35$. Calculated concentration profiles during swelling are shown in Fig. 5*B* for $\Phi_0 = 1$ vol% and 10 vol%. For both concentrations, it is found that swelling induces a strong local increase in PVA concentration in a thin layer close to the substrate surface. The critical concentration Φ_c was reached very rapidly within 1 μm of the substrate surface, after less than 1 and 0.1 s s for 1 vol% and 10 vol% solutions, respectively. For concentrations greater than 2.5 vol%, the predicted growth in hydrogel film thickness is in good agreement with the experiment (dashed lines in Fig. 4*C*) and is very similar to the results of the simple analytical model. For $\Phi_0 = 1$ vol%, simulations suggest that PVA hydrogel films still formed but were too thin to be detected with our setup.

Application Potential of Hydrogel Film Fabrication by Swelling-Induced Gelation. The versatility of the method was demonstrated by producing PVA hydrogel films with a variety of swelling polymer substrates: neutral chemical gels of PAAm, polyelectrolyte gels of PAAc–PAAm, as well as dry un–cross-linked films of poly(ethylene glycol) (PEG) (Fig. S5). For the latter, the substrate swells and eventually dissolves, which enables the formation of freestanding membranes of PVA hydrogel. To verify the generality of the approach, hydrogel films were also produced from aqueous solutions of poly(oxyethylene)-block-poly(oxypropylene)-block-poly(oxyethylene) (Pluronic F127), which form colloidal hydrogels above 15–20 wt% at 20 °C in water (Fig. S6*A*). Unlike with PVA, the so-obtained hydrogel films are not stable and eventually dissolve if they stay in solution. Alternatively, we verified that no hydrogel film is obtained if the polymer substrate swells in a polymer solution that does not exhibit a sol–gel transition like for PEG and poly(vinyl pyrrolidone) (PVP) solutions (Fig. S6 *C* and *D*).

One major practical interest of this approach lies in the possibility to incorporate other solutes to make functional coatings or films. For instance, the incorporation of osteoconductive hydroxyapatite particles into PVA hydrogel films has been shown to enhance cell adhesion to PVA hydrogels and stimulate osteoblast proliferation (30, 31). As an illustration, coatings of hydroxyapatite particles were produced by swelling-induced gelation on the same spherical PAAc–PAAm substrates as the ones studied above. The dry spheres were immersed in 10 wt% PVA aqueous solutions containing suspensions of nanoparticles or microparticles of hydroxyapatite. After 30–60 min of immersion and rinsing in water, the spheres were homogeneously coated with a white film (Fig. 6 *A* and *B*). Scanning electron microscopy (SEM) shows that both coatings consist of nanoparticles or microparticles embedded in a PVA matrix (Fig. 6 *D* and *E*). Conversely, no coating was formed if the substrate was swollen to equilibrium in water before immersion in the PVA–hydroxyapatite solutions (Fig. 6*C*).

The potential for cell encapsulation was demonstrated in another experiment adjusted to cell culture (Fig. S7 and *SI Materials and Methods*). Mouse fibroblasts (NIH 3T3 cell line) were dispersed in growth medium containing 10% (vol/vol) FBS and 12 wt% PVA. The solution was poured in wells containing dry un–cross-linked PEG substrates, which swelled and dissolved to produce freestanding PVA hydrogel films (Fig. S8). Such soluble substrates were selected to reduce the number of direct manipulations and ensure aseptic conditions during membrane rinsing, collection, and incubation. After 3-h incubation at 37 °C, these films were rinsed and incubated in growth medium (Fig. 6*F*). Due to sticking to the walls of the glass wells during swelling, they exhibited a gradient in thickness from 2 mm at the edges to 0.5 mm in the center (Fig. 6*G*). Epifluorescence observations show that cells were efficiently encapsulated in the PVA films (see Fig. S9 for positive and negative controls). Cells located too close to the interface with the PEG substrate did not survive,

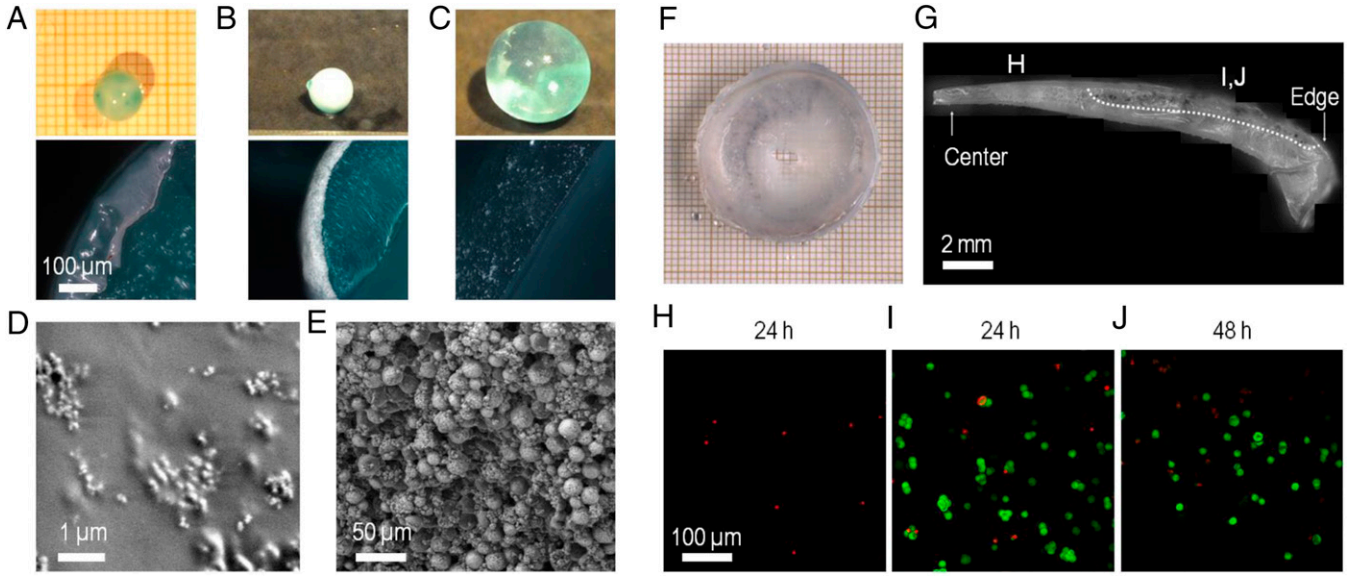

Fig. 6. Fabrication of composite ceramic-hydrogel coatings and cell encapsulation. (*A–E*) Fabrication of composite hydroxyapatite–PVA hydrogel coatings. (*A* and *B*) Coating by immersion of dry PAAc–PAAm spheres in 10 wt% PVA solutions containing dispersions of hydroxyapatite nanoparticles (5 wt%) (*A*) or microparticles (20 wt%) (*B*, *Top*) Pictures of spheres after immersion (30 min for nanoparticles, 60 min for microparticles) and rinsing in water (15 min). (*Bottom*) Cross-section images by optical microscopy. (*C*) Same observations as *B* showing the absence of coating when the PAAc–PAAm sphere is swollen to equilibrium in pure water before immersion in the PVA solution with hydroxyapatite microparticles. (*D* and *E*) Low-vacuum SEM observations of the surface of the spheres coated with nanoparticles (*D*) and with microparticles (*E*). (*F–J*) Encapsulation of mouse fibroblasts NIH 3T3 in PVA hydrogel films using swelling of dry PEG films. (*F*) Cell-laden PVA hydrogel film obtained after the encapsulation protocol. (*G*) Cross-section of the PVA hydrogel film showing the gradient in film thickness. The picture is constructed by juxtaposing several images. The bottom surface was in contact with the PEG substrate, and the top surface with the cell suspension. Dotted line delimitates the upper region where clusters of living cells are revealed by MTT staining. (*H–J*) Confocal microscopy observations near the top surface of the hydrogel films for different film thicknesses: less than 1-mm thickness after 24 h (*H*); more than 1-mm thickness after 24 h (*I*) and 48 h (*J*). Green staining by calcein reveals the cytoplasm of living cells. Red staining by ethidium reveals the nucleus of dead cells.

probably because of hypertonic conditions created during swelling (Fig. 6*H*). On the contrary, cells encapsulated further than 1.0 ± 0.5 mm from the PEG substrate remained alive with a viability of 70 ± 20% after 24 and 48 h (Fig. 6 *I* and *J*). 3-(4,5-Dimethylthiazol-2-yl)-2,5-diphenyltetrazolium bromide (MTT) staining revealed clusters of living cells and indicated the extent of the viability zone (Fig. 6*G*).

This experiment shows that there exists a range of conditions for which cells (fibroblasts) can be viably encapsulated by swelling-induced gelation. Depending on the cell type, sensitivity to hypertonic conditions and thus viability are expected to vary (32–34). The proposed approach offers many levers to modulate the microenvironment of encapsulated cells and therefore to control their viability and activity (35). For instance, the local gradient in osmotic pressure undergone during swelling can be reduced by changing the initial and equilibrium swelling ratios of the substrate as well as the PVA concentration; the cross-linking density and porosity of the PVA hydrogel might be adjusted by varying the PVA molecular weight or by mixing with other water-soluble polymers. More generally, incorporating bioactive additives in the PVA solution is another straightforward route to enhance the affinity of the encapsulated cells with the hydrogel matrix.

In conclusion, these results demonstrate that swelling of a hydrophilic polymer substrate in a polymer solution is a soft, autonomous, and finely tunable process to induce the growth of hydrogel films. Both experiments and simulations show that, even for rather dilute solutions (~1 wt%), high polymer concentrations are produced near the swelling surface. New synthesis or analytical methods based on such phenomenon could provide interesting low-energy alternative for polymer concentration and extraction, for example, without energy-intensive centrifugation steps. Furthermore, this autonomous mechanism opens fabrication routes, which may prove particularly valuable for biomedical and biological applications. The possibility to coat hydrogels with complex shapes and to incorporate bioactive compounds is a strong asset to tailor the biointegration of implants. The numerous advances in the design of autoassociative polymers (36), especially PVA modification (21, 37–40), and of nanocomposite hydrogels (41) are a boon to expand the range of attainable properties. With the possibilities to encapsulate cells and to produce freestanding membranes, one may also envision cost-effective and easy-to-implement methods for tissue engineering and 3D cell culture.

Materials and Methods

Materials. The chemicals used in this work were used as purchased without further purification. PVA aqueous solutions were fabricated from high–molecular-weight (89,000–98,000 g·mol^{-1}) and 99% hydrolyzed PVA (Sigma-Aldrich; 341584). The PAAm networks used as flat substrates were made from a 40 wt% aqueous solution of acrylamide (AAm) as the monomer, *N,N′*-methylenebisacrylamide (MBAAm) as the cross-linker with a ratio AAm/MBAAm of 37.5:1 (Sigma-Aldrich; A7168). Ammonium persulfate (APS) was used as the thermal initiator (Amresco; 0486) and *N,N,N′,N′*-tetramethylethylenediamine (TEMED) as the cross-linking accelerator (Sigma-Aldrich; T9281). Spherical substrates were made from commercially available PAAc–PAAm beads (Casa; Perles d'Eau). They were purchased in a swollen state composed of distilled water (99 wt%), sodium salt (0.2 wt%), and a network of acrylic acid (0.6 wt%) and acrylamide (0.2 wt%). Aqueous polymer solutions (10 wt%) were prepared from PEG (Mn = 3,400 g·mol^{-1}; Sigma-Aldrich), PVP (Mn = 40,000 g·mol^{-1}; Sigma-Aldrich), and Pluronic F127 (Mn = 12,600 g·mol^{-1}; Sigma-Aldrich). For more details on the materials, please see *SI Materials and Methods*.

Preparation of PVA Solutions. The PVA aqueous solutions were fabricated by dissolving PVA powder under mechanical stirring in ultrapure water using a silicon oil bath heated to 110 °C for 60 min. The weight of the solutions was measured before and after dissolution, and water was added to correct from evaporation. After stirring, the solutions were covered and let cool down and degas. Six solutions were prepared with theoretical PVA concentration

of 1, 2.5, 5, 7.5, 10, and 15 wt%. Actual concentrations measured a posteriori by water evaporation were 1.0, 2.6, 5.3, 7.6, 10.6, and 14.7 wt%, respectively. These latter values were used for fitting by the model.

Fabrication of Swelling Substrates. The flat PAAm substrates were prepared from a 12 vol% aqueous solution of AAm–MBAAm obtained by dilution of the commercial 40 wt% solution in ultrapure water. Synthesis was done by mixing this solution with of a 10 wt% aqueous solution of APS at 2 vol% and TEMED at 0.2 vol%. The whole solution was stirred by magnetic stirrer and poured in a glass mold of $100 \times 130 \times 5$ mm^3. The mold was kept at 20 °C for 2 h to obtain cross-linking. The obtained PAAm gel film was cut into 2×4 cm^2 rectangular pieces and dried at 20 °C in air under extractor hood for 24 h. The spherical PAAc–PAAm substrates were obtained from swollen PAAc–PAAm beads that were dried under extractor hood for 24 h.

Stability of Hydrogel Films. PVA hydrogel films were fabricated by immersing dry 3-mm-thick rectangular PAAm substrates in a 15 wt% PVA aqueous solution for 3 h. After immersion, the swollen substrates were removed from the PVA solution and were vigorously washed in a large excess of ultrapure water for 15 min. Hydrogel films were then peeled off from the substrate surface, attached to fishhooks, and stored in glass tubes filled with ultrapure water. Pictures of the films were taken with a camera (D300s; Nikon) right after fabrication, after 1-h and 1-wk storage at 20 °C or after 1-h storage in an oil bath at 90 °C.

Measurement of Hydrogel Film Growth. The formation and growth of hydrogel films at the surface of swelling spherical substrates was observed with a macroscope (M420 Wild-Leitz; Leica). Spherical PAAc–PAAm substrates were placed in Petri dishes filled with ultrapure water or PVA aqueous solutions with different concentrations. The Petri dishes were placed on a *X*–*Y* translation stage. Two lighting methods were used separately to distinguish the hydrogel film and the substrate surface boundaries (Fig. S4). In-lens lighting was used to reveal the surfaces of the hydrogel film. Lighting in the plane of the image revealed the boundary of the substrate surface only. The formation and growth of hydrogel films was recorded during 24 h with a first measurement after 2 min of immersion. At each time point, images were recorded with the two types of lighting. Film thickness was estimated by subtracting the radius of the PAAc–PAAm sphere (Fig. S4*B*) to the radius of the film around the PAAc–PAAm sphere (Fig. S4*A*). Measurements were repeated on two to five beads for each time point. Data points in Fig. 4 are represented as the mean with SD as the error bar.

For more details about the methods, in particular, X-ray scattering, fabrication of ceramic coatings, and cell encapsulation, please see *SI Materials and Methods*.

ACKNOWLEDGMENTS. We thank Y. Auriac for technical assistance on experiment design, M. Betbeder and F. Gaslain for assistance in electron microscopy, C. Mocuta and H. Proudhon for assistance on synchrotron experiments, and S. Tencé-Girault for X-ray analysis. We also thank L. Tsagris for assistance on cell encapsulation experiments and J.-M. Petit for epifluorescence microscopy. We thank L. Leibler for encouragement and interpretations on gel swelling, M. Cloître and R. Fournier for discussions on associative polymers, and D. J. Pine and R. Nicolaÿ for discussions and critical review of the manuscript. D.M. acknowledges a PhD scholarship from MINES ParisTech. The financial support of MINES ParisTech, ESPCI Paris, and Institut Carnot Mines (Grant HAP-Process 2012) is acknowledged.

1. Boateng JS, Matthews KH, Stevens HNE, Eccleston GM (2008) Wound healing dressings and drug delivery systems: A review. *J Pharm Sci* 97(8):2892–2923.
2. Lih E, Oh SH, Joung YK, Lee JH, Han DK (2015) Polymers for cell/tissue anti-adhesion. *Prog Polym Sci* 44:28–61.
3. Slaughter BV, Khurshid SS, Fisher OZ, Khademhosseini A, Peppas NA (2009) Hydrogels in regenerative medicine. *Adv Mater* 21(32-33):3307–3329.
4. Baker MI, Walsh SP, Schwartz Z, Boyan BD (2012) A review of polyvinyl alcohol and its uses in cartilage and orthopedic applications. *J Biomed Mater Res B Appl Biomater* 100(5):1451–1457.
5. Tibbitt MW, Anseth KS (2009) Hydrogels as extracellular matrix mimics for 3D cell culture. *Biotechnol Bioeng* 103(4):655–663.
6. Lutolf MP, Hubbell JA (2005) Synthetic biomaterials as instructive extracellular microenvironments for morphogenesis in tissue engineering. *Nat Biotechnol* 23(1):47–55.
7. Malda J, et al. (2013) 25th anniversary article: Engineering hydrogels for biofabrication. *Adv Mater* 25(36):5011–5028.
8. Nicodemus GD, Bryant SJ (2008) Cell encapsulation in biodegradable hydrogels for tissue engineering applications. *Tissue Eng Part B Rev* 14(2):149–165.
9. Mertaniemi H, et al. (2016) Human stem cell decorated nanocellulose threads for biomedical applications. *Biomaterials* 82:208–220.
10. Peters A, Candau SJ (1988) Kinetics of swelling of spherical and cylindrical gels. *Macromolecules* 21(7):2278–2282.
11. Doi M (2009) Gel dynamics. *J Phys Soc Jpn* 78(5):52001.
12. Budtova T, Navard P (1996) Swelling dynamics of cross-linked poly(acrylic acid) and neutralized poly(acrylate-co-acrylic acid) in aqueous solutions of (hydroxypropyl) cellulose. *Macromolecules* 29(11):3931–3936.
13. Packter A, Nerurkar M (1968) Crystallization in films of polar vinyl polymers—I. Crystallinity of polyvinyl alcohol films prepared by evaporation of aqueous solutions. *Eur Polym J* 4(6):685–693.
14. Kawanishi K, Komatsu M, Inoue T (1987) Thermodynamic consideration of the sol-gel transition in polymer solutions. *Polymer (Guildf)* 28(6):980–984.
15. Young T-H, Yao N-K, Chang R-F, Chen L-W (1996) Evaluation of asymmetric poly(vinyl alcohol) membranes for use in artificial islets. *Biomaterials* 17(22):2139–2145.
16. Barzin J, Madaeni SS, Pourmoghadasi S (2007) Hemodialysis membranes prepared from poly(vinyl alcohol): Effects of the preparation conditions on the morphology and performance. *J Appl Polym Sci* 104(4):2490–2497.
17. Cascone MG, Laus M, Ricci D, Del Guerra RS (1995) Evaluation of poly(vinyl alcohol) hydrogels as a component of hybrid artificial tissues. *J Mater Sci Mater Med* 6(2): 71–75.
18. Vrana NE, et al. (2012) Cell encapsulation and cryostorage in PVA-gelatin cryogels: Incorporation of carboxylated ε-poly-L-lysine as cryoprotectant. *J Tissue Eng Regen Med* 6(4):280–290.
19. Hassan CM, Peppas NA (2000) Structure and applications of poly(vinyl alcohol) hydrogels produced by conventional crosslinking or by freezing/thawing methods. *Biopolymers · PVA Hydrogels, Anionic Polymerisation Nanocomposites* (Springer, Berlin), pp 37–65.
20. Otsuka E, Suzuki A (2009) A simple method to obtain a swollen PVA gel crosslinked by hydrogen bonds. *J Appl Polym Sci* 114(1):10–16.
21. Jensen BEB, et al. (2011) Poly(vinyl alcohol) physical hydrogels: Noncryogenic stabilization allows nano- and microscale materials design. *Langmuir* 27(16):10216–10223.
22. Watase M, Nishinari K (1985) Rheological and DSC changes in poly(vinyl alcohol) gels induced by immersion in water. *J Polym Sci Polym Phys Ed* 23(9):1803–1811.
23. Willcox PJ, et al. (1999) Microstructure of poly(vinyl alcohol) hydrogels produced by freeze/thaw cycling. *J Polym Sci B Polym Phys* 37(24):3438–3454.
24. Bastide J, Candau S, Leibler L (1981) Osmotic deswelling of gels by polymer solutions. *Macromolecules* 14(3):719–726.
25. Bercea M, Morariu S, Rusu D (2013) In situ gelation of aqueous solutions of entangled poly(vinyl alcohol). *Soft Matter* 9(4):1244–1253.
26. Barrière B, Leibler L (2003) Kinetics of solvent absorption and permeation through a highly swellable elastomeric network. *J Polym Sci B Polym Phys* 41(2):166–182.
27. Hara C, Matsuo M (1995) Phase separation in aqueous poly(vinyl alcohol) solution. *Polymer (Guildf)* 36(3):603–609.
28. Holloway JL, Lowman AM, Palmese GR (2013) The role of crystallization and phase separation in the formation of physically cross-linked PVA hydrogels. *Soft Matter* 9(3): 826–833.
29. Cussler E (2009) *Diffusion: Mass Transfer in Fluid Systems* (Cambridge Univ Press, Cambridge, UK), 3rd Ed.
30. Hou R, et al. (2013) Magnetic nanohydroxyapatite/PVA composite hydrogels for promoted osteoblast adhesion and proliferation. *Colloids Surf B Biointerfaces* 103: 318–325.
31. Hayami T, Matsumura K, Kusunoki M, Nishikawa H, Hontsu S (2007) Imparting cell adhesion to poly(vinyl alcohol) hydrogel by coating with hydroxyapatite thin film. *Mater Lett* 61(13):2667–2670.
32. Woods EJ, Zieger MAJ, Lakey JRT, Liu J, Critser JK (1997) Osmotic characteristics of isolated human and canine pancreatic islets. *Cryobiology* 35(2):106–113.
33. Zawlodzka S, Takamatsu H (2005) Osmotic injury of PC-3 cells by hypertonic NaCl solutions at temperatures above 0 °C. *Cryobiology* 50(1):58–70.
34. Cai Q, et al. (2005) Pax2 expression occurs in renal medullary epithelial cells in vivo and in cell culture, is osmoregulated, and promotes osmotic tolerance. *Proc Natl Acad Sci USA* 102(2):503–508.
35. Stevens MM, George JH (2005) Exploring and engineering the cell surface interface. *Science* 310(5751):1135–1138.
36. Tsitsilianis C (2010) Responsive reversible hydrogels from associative "smart" macromolecules. *Soft Matter* 6(11):2372–2388.
37. Nuttelman CR, Henry SM, Anseth KS (2002) Synthesis and characterization of photocrosslinkable, degradable poly(vinyl alcohol)-based tissue engineering scaffolds. *Biomaterials* 23(17):3617–3626.
38. Schmedlen RH, Masters KS, West JL (2002) Photocrosslinkable polyvinyl alcohol hydrogels that can be modified with cell adhesion peptides for use in tissue engineering. *Biomaterials* 23(22):4325–4332.
39. Sailaja GS, Sreenivasan K, Yokogawa Y, Kumary TV, Varma HK (2009) Bioinspired mineralization and cell adhesion on surface functionalized poly(vinyl alcohol) films. *Acta Biomater* 5(5):1647–1655.
40. Arai K, Okuzono M, Shikata T (2015) Reason for the high solubility of chemically modified poly(vinyl alcohol)s in aqueous solution. *Macromolecules* 48(5):1573–1578.
41. Schexnailder P, Schmidt G (2009) Nanocomposite polymer hydrogels. *Colloid Polym Sci* 287(1):1–11.
42. Bunn CW (1948) Crystal structure of polyvinyl alcohol. *Nature* 161(4102):929–930.